

**PAPER**

# Implementation of physiological fluids to provide insight into the characterization, fate, and biological interactions of silver nanoparticles

To cite this article: Emily K Breitner *et al* 2018 *Nanotechnology* **29** 254001

View the [article online](#) for updates and enhancements.

# Implementation of physiological fluids to provide insight into the characterization, fate, and biological interactions of silver nanoparticles

Emily K Breitner<sup>1</sup>, Katherine E Burns<sup>1</sup>, Saber M Hussain<sup>2</sup> and Kristen K Comfort<sup>1</sup> 

<sup>1</sup>Department of Chemical and Materials Engineering, University of Dayton, Dayton, OH 45469, United States of America

<sup>2</sup>Molecular Bioeffects Branch, Airmen Systems Directorate, 2728 Q St, Building 837, Wright-Patterson Air Force Base, OH 45433, United States of America

E-mail: [Kcomfort1@udayton.edu](mailto:Kcomfort1@udayton.edu)

Received 2 December 2017, revised 8 March 2018

Accepted for publication 4 April 2018

Published 25 April 2018



CrossMark

## Abstract

Silver nanoparticles (AgNPs) are being increasingly utilized in consumer and medical applications. However, there remains conflicting reports on their safety, which are evaluated through a combination of *in vitro* and *in vivo* exposure models. These discrepancies may arise, in part, due to the inherent differences between cell-based and animal systems. It is well established that nanotoxicological effects are highly dependent on the unique physicochemical properties and behavior of the particle set, including size, surface chemistry, agglomeration, and ionic dissolution. However, recent studies have identified that these properties vary as a function of exposure environment; providing a rationale for the contradictory results between *in vitro* and *in vivo* assessments. Artificial physiological fluids are emerging as a powerful tool as they allow for the characterization of NPs in an environment which they would likely encounter *in vivo*, in addition to having the experimental advantages of flexibility and consistency. Here, we demonstrated that the utilization of artificial fluids provided a mechanism to assess AgNP behavior and induced bioresponses in environments that they would likely encounter *in vivo*. AgNPs were introduced within an alveolar-based exposure model, which included alveolar epithelial (A549) cells incubated within artificial alveolar fluid (AF). Additionally, the particles underwent extensive characterization within both AF and lysosomal fluid, which the AgNPs would encounter following cellular internalization. Following incubation in physiological environments AgNP properties were significantly modified versus a traditional media environment, including alterations to both extent of agglomeration and rate of ionic dissolution. Moreover, when A549s were exposed to AgNPs in AF, the cells displayed lower cytotoxicity and stress rates, corresponding to a fluid-dependent drop in silver ion production. This work highlights the need for enhanced *in vitro* models that more closely mimic *in vivo* exposure environments in order to capture true NP behaviors and cellular interactions.

Keywords: alveolar fluid, enhanced *in vitro* model, ionic dissolution, nano-cellular interface

(Some figures may appear in colour only in the online journal)

## 1. Introduction

In recent years, nanoparticles (NPs) have been increasingly utilized due to their unique physicochemical properties, which differ from those of bulk materials [1]. These distinctive parameters, which include increased surface area and reactivity, unique plasmonic behaviors, and the ability to precisely design characteristics such as size, morphology, and surface chemistry, make NPs advantageous in consumer, medical, agricultural, and military sectors [2, 3]. However, concerns exist regarding the safety of NPs following human exposure, which can occur inadvertently through inhalation, skin absorption, or ingestion [4, 5]. Alternatively, exposure can be deliberate, as NPs are being explored for biomedical applications, such as drug delivery, cancer therapeutics, and bioimaging [6, 7]. Regardless of exposure mechanism, it is necessary to fully elucidate the behavior and interactions of NPs within biological systems prior to their widespread utilization, in order to verify their safety.

Currently, silver NPs (AgNPs) are employed in hundreds of consumer and medical applications due to their robust antimicrobial and unique optical properties [8, 9]. AgNPs are particularly attractive to the medical field, with current applications including devices, material coatings, bandages, and wound dressings [3]. Additionally, AgNPs are found in a vast array of consumer products spanning detergents, clothing, cosmetics, air sanitizers, and food storage containers [10]. Despite their many positive attributes, AgNPs have been associated with negative toxicological effects, including activation of cytotoxicity, intracellular stress, inflammatory response, and genetic modifications [3, 10, 11]. Previous studies have shown that AgNPs predominantly induce these responses via a reactive oxygen species (ROS) dependent mechanism, which ultimately leads to an overwhelming and unrecoverable stress response [12, 13].

Previous reports have demonstrated that NP-induced bioresponses are directly dependent upon unique physicochemical properties, including size, surface chemistry, composition, and morphology [1]. Primary AgNP size has been shown to influence ROS generation and subsequent cytotoxicity, with smaller AgNPs initiating greater stress levels compared to their larger counterparts [13, 14]. Additionally, it has been established that deposition rates correlate to cellular responses, with augmented nano-cellular interactions producing a higher degree of cytotoxicity [14, 15]. Recently, it has been shown that ionic dissolution of AgNPs is a major contributor to observed cytotoxic outcomes, with higher rates of silver ion production resulting in increased toxicity, intracellular stress levels, and modifications to cell functionality [16, 17]. As such, characterizing particle behavior in a biological environment, including quantification of ion generation, may help predict the degree of AgNP biocompatibility.

It is becoming increasingly recognized that physicochemical properties and behavior of NPs are a function of surrounding environmental factors, such as fluid composition, cellular architecture, and fluid dynamic conditions [17–19]. For example, within the acidic environment of lysosomal fluid (LF), the rate of AgNP ionic dissolution was

substantially increased versus a media environment [17]. As ion production is linked to cytotoxic potential of AgNPs, characterization within a physiologically relevant environment may improve prediction of cellular responses following exposure. However, there exists a knowledge gap pertaining to how these environmental factors, such as exposure fluid pH and composition, modify NP behavior, potentially contributing to the observed discrepancies between *in vivo* and *in vitro* safety assessments [20].

*In vitro* studies are often utilized for NP safety screenings owing to their experimental flexibility, reproducibility, and lower cost investment [21, 22]. However, standard cellular-based models have drawn criticism due to their limited relevance to *in vivo* environmental conditions [23]. This can be partially traced back to the fact that culture media is not representative of the different types of physiological environments that NPs would encounter in a human body, such as interstitial, alveolar, and LFs. Alveolar fluid (AF) is a surfactant produced by type II alveolar cells and is responsible for protecting the alveoli endothelium and facilitating gas transfer in the lungs by reducing surface tension during respiration. As AF also serves to trap foreign material following inhalation, it has emerged as a likely fluid AgNPs would encounter in the human body. Following cellular internalization via numerous endocytosis mechanisms, NPs are transitioned to lysosomes for targeted destruction [24, 25]. The fluid within the lysosomes, LF, contains numerous enzymes and has an acidic pH of 4.5, both of which contribute the effective destruction of internalized materials. As such, LF is both an environment frequently encountered by NPs and has the potential to substantially alter NP properties and behaviors, including ion production.

The inclusion of artificial physiological fluids within *in vitro* environments allows for a more reliable, reproducible, and accurate exposure model; thereby improving the predictive potential for evaluation of NP safety and therapeutic efficacy [17, 19]. Utilization of biological fluids have the added benefit of post-exposure NP recovery, allowing for characterization within a more-relevant, physiological environment [26]. Preliminary studies have uncovered modifications to both behavior and cellular responses when NP exposure occurred within relevant biological fluids. For instance, when gold nanorods were dispersed in alveolar, cerebrospinal, or interstitial fluids, extensive agglomeration occurred. This augmented aggregation correlated with a loss of photothermal potential due to a reduction in available surface area [27]. Extensive agglomeration was also observed within AF and interstitial fluid for gold and copper NPs, respectively [28, 29]. These fluid-dependent modifications resulted in modified nano-cellular interfaces and deposition efficiencies. Moreover, NP exposure in biological fluids modified the protein corona composition, deposition, and cytotoxicity versus traditional cell culture medium [19]. Taken together, these studies demonstrate that fluid composition influence NP behavior and dependent bioresponses within *in vitro* systems and that artificial fluids are a valuable tool in these assessments.

Therefore, the goal of this study was to expand on these previous efforts to further explore and characterize the impact of AF and LF on the physicochemical properties and behavior of AgNPs. Polyvinylpyrrolidone (PVP) coated AgNPs, which are renowned for their stability, were specifically selected for this study as there exists a significant knowledge gap regarding the ability of physiological fluids to modify PVP NPs. Additionally, the impact of an AF exposure model on the nano-cellular interface and AgNP safety assessments were explored, which to date has not been examined. Experimentation was carried out using an A549, lung epithelial model, as inhalation is a primary mode of exposure [4, 5]. AF and LF were implemented as they are two likely environments AgNPs would encounter *in vivo*. This study demonstrated that physiological fluids were capable of introducing serious alterations to AgNP physicochemical properties, which in turn modified particle dosimetry, the rate of ionic dissolution, and target biological responses. Moreover, this work highlights how physiological fluids can mimic *in vivo* exposure environments, thereby improving the relevance of *in vitro* models for NP safety assessments.

## 2. Materials and methods

### 2.1. Cell culture

The human alveolar epithelial, A549, cell model was purchased from American Type Cell Culture and utilized in this study. A549 cells were maintained in RPMI 1640 media supplemented with 10% fetal bovine serum (FBS) and 1% antibiotics. The cells, grown in tissue-culture treated petri dishes, were housed in a humidified incubator at 37 °C and 5% CO<sub>2</sub>.

### 2.2. Composition of artificial fluids

In this study, artificial AF and LF served as the biologically relevant exposure environments. These fluid solutions were synthesized using previously reported recipes by Stopford *et al* [30], which were designed to accurately mimic true physiological fluids. AF, with a pH of 7.4, was comprised of numerous salts, supplemented with the lipid phosphatidyl choline. Artificial LF combined a variety of salts, formaldehyde, glycerin, and was adjusted to an acidic pH of 4.5. As neither AF nor LF contained proteins, 1% FBS was added to maintain basic cell functionality and improve physiological relevance.

### 2.3. AgNPs and characterization

The PVP-coated, 75 nm AgNPs were purchased from nano-Composix in concentrated liquid form. The AgNPs were stored in the dark at 4 °C, in accordance with manufacturer recommendations, to minimize NP alterations throughout the course of this study. Primary particle size and morphology were determined via transmission electron microscopy (TEM), on a Hitachi H-7600. TEM images were used to

determine the primary size of the AgNPs through ImageJ analysis.

For all other characterization assessments, fresh AgNP stocks were generated by dilution to a final concentration of 25 µg ml<sup>-1</sup> in the denoted fluid–water, cell culture media, AF, or LF. AgNP spectral profiles were generated using ultra-violet–visible (UV–vis) spectroscopy on a Synergy 4 BioTek microplate reader. The degree of NP agglomeration was quantified using dynamic light scattering (DLS) on an Anton Paar Litesizer 500. The surface charge, as assessed through zeta potential measurement, was also carried out using the Litesizer 500, for each experimental fluid.

To assess AgNP dissolution, the particles were suspended in each fluid for 24 h at 37 °C. The AgNPs were removed from the solution via centrifugation at 10 000 rpm for 15 min and the ion containing supernatant was collected. The silver content within the liquid supernatant was measured via inductively coupled plasma mass spectrometry (ICP-MS) on a Perkin Elmer NexION 300D. The dissolution percentage was calculated based off the original 25 µg ml<sup>-1</sup> AgNP concentration.

### 2.4. AgNP deposition analysis

A549 cells were seeded into a 6 well plate at a concentration of 8 × 10<sup>5</sup> cells per well in media and returned to the incubator to allow for cellular attachment. The next day the cells were washed and dosed with 5 µg ml<sup>-1</sup> AgNPs, in either media or AF, and returned to the incubator. After a 24 h exposure period, the A549 cells were washed, removed from the plate using trypsin, counted, and digested with a mixture containing 0.05% Triton X-100, 3% HCl, and 1% HNO<sub>3</sub>. The intracellular silver concentration was determined via ICP-MS on the NexION 300D. Deposition percentages were calculated against the administered (5 µg ml<sup>-1</sup>) dosage.

### 2.5. Visualization of the nano-cellular interface

The A549 cells were plated into a 2-well chambered slide at a density of 2 × 10<sup>5</sup> cells per chamber and returned to the incubator. The following day, the cells were washed and exposed to the denoted conditions, which include a combination of AgNPs, media, or AF. After an exposure duration of 24 h, the cells were washed, fixed with 4% paraformaldehyde, and prepared for fluorescence microscopy. The cells underwent actin and nuclear staining using Alex Fluor 555-phalloidin and 4',6-diamidino-2-phenylindole (DAPI), respectively, both of which were purchased from Thermo Fisher Scientific. The chambers were removed and the slides were imaged using an Olympus BX41 microscope and QCapture Pro Imaging software (Aetos Technologies).

### 2.6. Cellular response to AgNP exposure

A549s were plated into a 96-well plate at a concentration of 4 × 10<sup>4</sup> cells per well in media and incubated overnight. The cells were then washed and exposed to the denoted conditions for an additional 24 h, followed by analysis for cellular viability and stress, as assessed via lactate dehydrogenase (LDH)

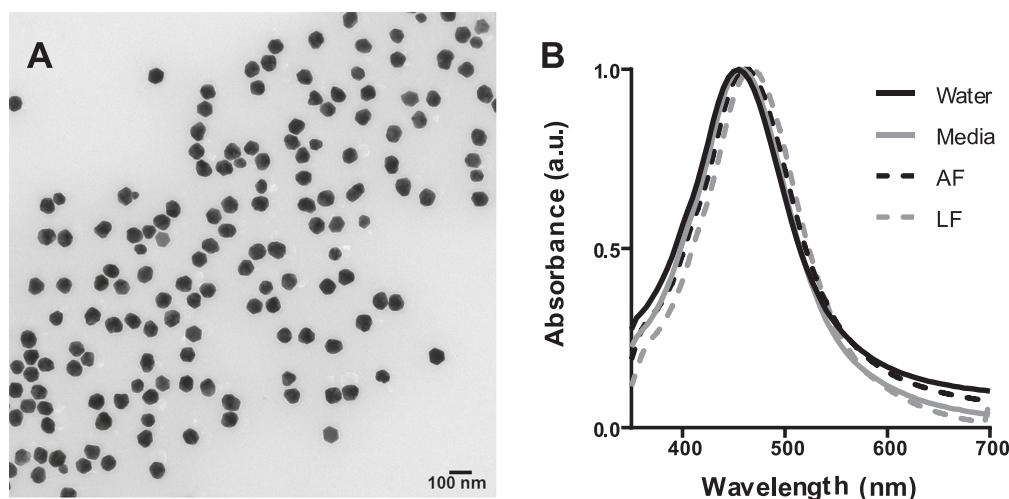


**Figure 1.** AgNP characterization. (A) Representative TEM image of the AgNPs demonstrated a predominant spherical morphology. Additionally TEM images were used to determine a primary size of  $82.4 \pm 5.5$  nm. (B) UV-vis generated spectral profiles of the AgNPs following incubation in the experimental fluids.

release and ROS, respectively. As the acidic nature of LF is not biocompatible for cellular incubation, only AF was examined for these endpoints.

Released LDH was quantified using the CytoTox 96 Nonradioactive cytotoxicity assay (Promega). Percent viability following AgNP exposure was determined using a negative (untreated media) and a positive control, consisting of lysed A549 cells. Intracellular ROS levels within A549 cells were monitored using the DCFH-DA probe (Thermo Fisher Scientific). ROS experimental values were normalized against untreated, media samples. All experimentation included fluid only exposure conditions to ensure that AF fluid incubation did not elicit a biological response. Both LDH and ROS procedures were carried out in accordance with the manufacturer's instructions.

### 2.7. Statistical analysis

All data is presented as the mean  $\pm$  the standard error of the mean. For all experiments, three independent trials were performed. For AgNP characterization and deposition, a one-way ANOVA with Bonferroni post-test was carried out using GraphPad Prism. A two-way ANOVA with Bonferroni post-test was performed for A549 viability and ROS evaluations. For all experimentation, a *p*-value threshold of 0.05 was used to determine statistical significance.

## 3. Results and discussion

### 3.1. Exposure to physiological fluids altered AgNP characteristics

PVP-coated, AgNPs were specifically selected for this study owing to their high utilization in applications that result in human exposure, such as clothing additives, antimicrobial sprays, and sterile bandages [3, 10]. In addition to its known improvement of particle stability [31], PVP surface chemistry

was chosen due to the fact that there is a lack of knowledge regarding the ability of physiological fluids to modify PVP NPs. As it is established that physicochemical properties are a predominant influence in the safety of AgNPs, the experimental NPs first underwent a full characterization analysis [1]. Moreover, as environmental influences can modify characteristics and behaviors, these characterization assessments were carried out following AgNP dispersion in AF and LF, in addition to media and water.

Figure 1(A) shows a representative TEM image of the 75 nm AgNPs. From this image a general spherical morphology and uniformity of the particles can be seen. Using multiple TEM images and ImageJ software analysis, a primary particle size of  $82.4 \pm 5.5$  nm was determined. While the morphology of the AgNPs are predominantly spherical, there are a few examples of particles that display shapes, such as hexagon and pentagons. While different morphologies can elicit differential behaviors and cellular responses, these modifications are relatively minor as determined by the small standard deviation. Moreover, as the same particle stock was used throughout experimentation, any morphological alterations would be consistent throughout this study. Next, the AgNP spectral profile was visualized following dispersion in each experimental fluid (figure 1(B)). The spectral profiles contained a single, sharp peak, which is indicative of a uniform NP stock, further supporting the TEM data. When evaluated in AF or LF, there was a slight right-shift in the peak absorbance wavelength, which typically arises due to increased particle agglomeration.

To quantify the extent of AgNP agglomeration within each fluid environment, the samples underwent DLS analysis (figure 2(A)). These results demonstrated a significant increase in inter-particle association within AF and LF versus media, with LF producing a final agglomerate size nearly twice as large. These results are in agreement with the observed right-shift of the spectral profiles and with the literature [28, 29]. While there is a slight increase in size within media, this is due to the formation of a protein corona, which

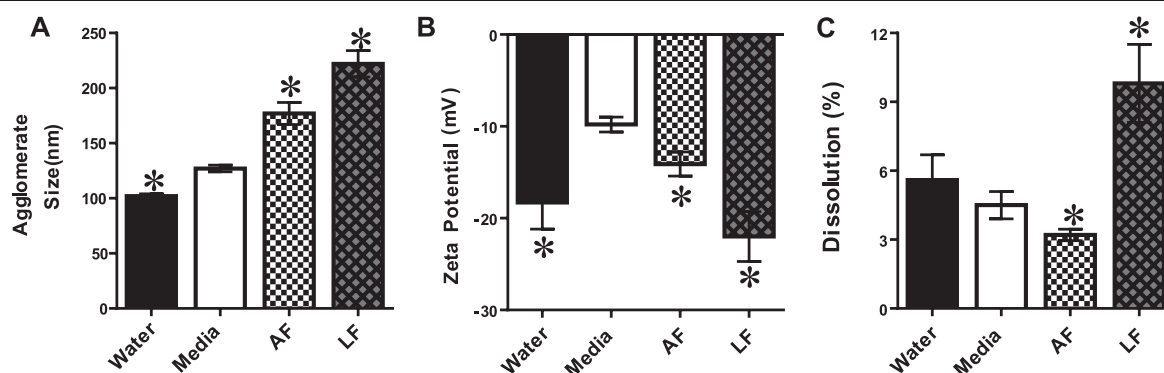


**Figure 2.** Characterization of AgNP behavior as a function of environmental composition. (A) DLS analysis was utilized to determine the AgNP agglomerate size following incubation in varying fluid environments. (B) Following dispersion in the different experimental fluids, the surface charge of the AgNPs was assessed via zeta potential measurement. (C) After a 24 h incubation, the extent of AgNP ionic dissolution was determined for each exposure fluid. Data represents 3 independent trials with \* denoting statistical significance from media conditions ( $p < 0.05$ ).

instantaneously forms around NPs in high protein environments [32, 33]. In addition to agglomeration, the surface charge of the AgNPs within each fluid was determined via zeta potential analysis (figure 2(B)). As expected, surface charge was found to slightly vary with fluid environment, in accordance with the fluid composition.

Next, the extent of ionic dissolution was analyzed following incubation in each experimental fluid, as ion production has been shown to be a major contributor to the cytotoxic potential of AgNPs [34]. As seen in figure 2(C), the general trend was that ion production decreased with increasing agglomerate size, due to a corresponding reduction in exposed surface area. The exception to this was a significantly increased rate of ionic dissolution following AgNP incubation in LF. As LF is acidic, this increase in ion production is not surprising, owing to the ability of acidic solutions to dissolve solid metals into ionic form [35]. Taken together, these results demonstrated that AgNP exposure within biological fluids altered their behavioral patterns, including modified agglomeration and ionic dissolution; both of which can impact the cellular interactions and subsequent biological responses.

### 3.2. Replacement of cell culture media with AF modified the AgNP-A549 interface

The next goal was to assess to if replacing traditional cell culture media with AF impacted the nano-cellular interface. The first step was to ensure that the A549 cells could successfully thrive within an AF environment. As shown in figure 3, A549 cells were successfully maintained for 24 h in AF, although a visible change in cellular morphology occurred. AF incubated cells (figure 3(B)) demonstrated a curved cellular membrane, versus the more globular nature associated with the media environment (figure 3(A)). We hypothesize that this curvature is due to the excess phosphatidyl choline, which could associate with the extracellular membrane.

Next, A549 cells were exposed to AgNPs within either a media or AF environment (figures 3(C) and (D)). As before,

the curved cellular morphology was associated with AF incubation. In both images, AgNPs are seen interacting with the A549 cells, demonstrating particle deposition. However, when comparing extent of AgNP interactions between fluid environments, it appears that AF exposure resulted in greater deposition, as denoted with more visible particles. While some larger white clumps are associated with AF, which would indicate extensive agglomeration and sedimentation, the majority of AgNPs appear well-dispersed, in agreement with the previous DLS data (figure 2(A)).

In order to confirm that AF exposure conditions correlated with increased nano-cellular interactions, AgNP deposition efficiencies were determined quantitatively for both exposure models. As seen in figure 4, the deposition efficiency in media was approximately 18%, which while low is not unexpected due to the increased stability associated with PVP. However, when AgNPs were introduced into the AF culture, the deposition efficiency increased slightly to approximately 25%. This greater deposition rate is likely due to the fluid-dependent increase in AgNP agglomerate size, as larger aggregates would be subjected to more significant sedimentation forces [36].

### 3.3. Differential A549 stress and toxicity responses

As it was previously identified that AF incubation altered both the physiochemical characteristics and AgNP-A549 interactions, the next goal was to assess if these modifications translated to differential biological responses. As it is well established that AgNPs induce cytotoxicity through an ROS mechanism, these endpoints were selected for evaluation [12, 13, 37]. In addition to evaluating A549 viability and stress response following AgNP exposure, fluid-specific controls were included to ensure that any observed modifications were due to NP behavior, and not an artifact of the fluid itself (figures 5(A) and 6(A)). These results verified that whether maintained in media or AF, A549 cells demonstrated negligible toxicity and equivalent basal ROS levels. Additionally, these results confirmed that AF did not interfere with assay performance, meaning that any difference in

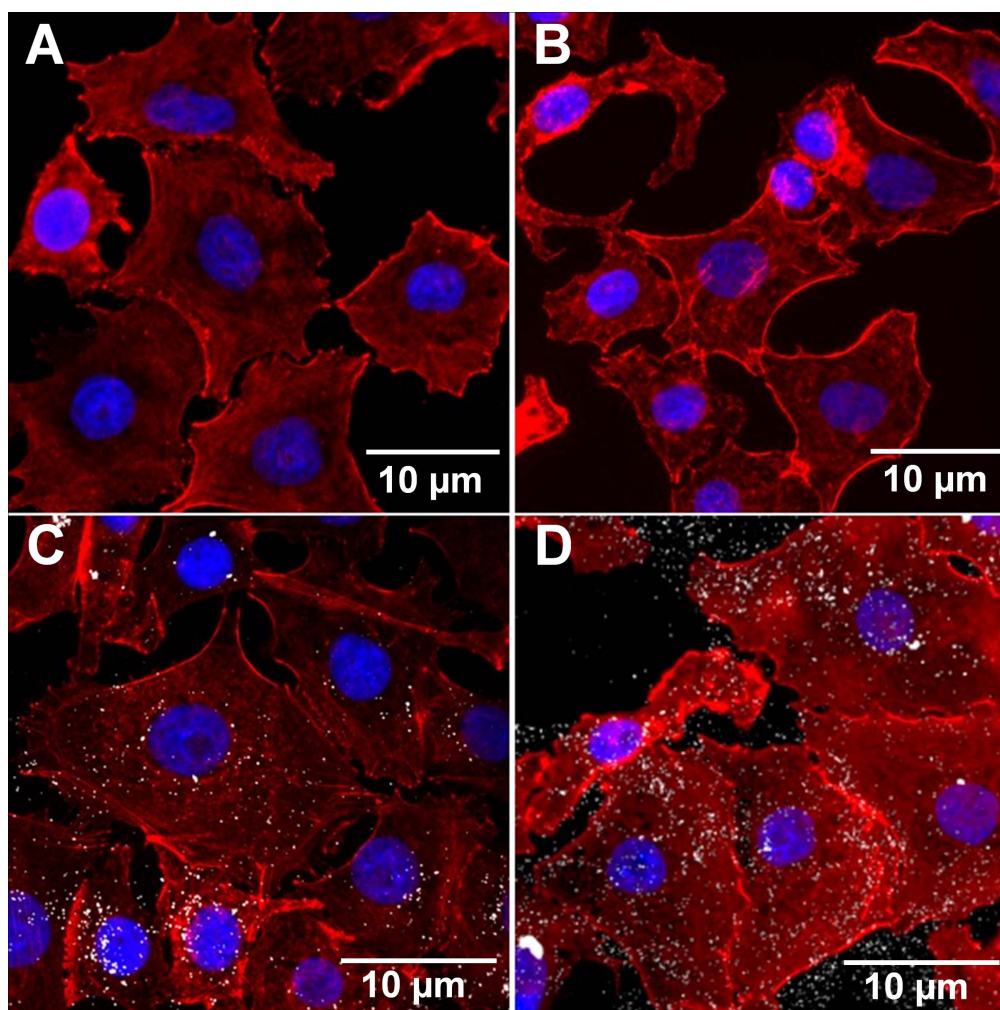


**Figure 3.** Visualizing the AgNP-A549 interface. Representative fluorescent images are shown following a 24 h incubation of A549 cells under the conditions of (A) media without AgNPs, (B) AF without AgNPs, (C) media with  $5 \mu\text{g ml}^{-1}$  AgNPs, and (D) AF with  $5 \mu\text{g ml}^{-1}$  AgNPs. In these images the A549 cells underwent actin (red) and nuclear (blue) staining with AgNPs appearing as white.

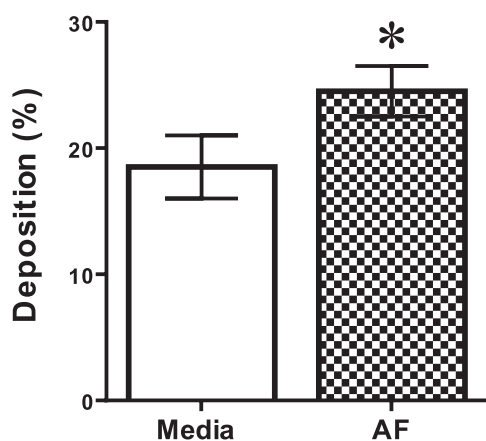


**Figure 4.** AgNP deposition efficiency. A549 cells were exposed to  $5 \mu\text{g ml}^{-1}$  AgNPs for 24 h in either traditional cell culture media or alveolar fluid (AF). The deposition efficiency, the percentage of administered AgNPs that were either internalized by or tightly bound to the cells, was determined via ICP-MS. Data represents 3 independent trials with \* denoting statistical significance from media conditions ( $p < 0.05$ ).

bioresponses that arose between media and AF environments were due to AgNP modifications.

Looking first at A549 viability (figure 5), as expected, increasing AgNP exposure dosages resulted in a corresponding rise in cytotoxicity within a standard media environment. At the greatest AgNP exposure concentration,  $25 \mu\text{g ml}^{-1}$ , significant A549 death transpired, approximately 40%. When the same dose-dependent assessment was carried out in an AF environment, a stepwise viability response still occurred. However, when directly comparing fluids, AF produced a significantly lower toxic response at  $25 \mu\text{g ml}^{-1}$  versus media exposure.

As AgNPs induce cytotoxicity through an oxidative stress mechanism, the LDH results were confirmed through assessment of intracellular ROS production (figure 6). Similar to the cytotoxicity data, an AgNP dose-dependent increase in ROS was identified in media. These augmented ROS levels correlated to the observed AgNP-induced toxicity. Additionally, within the AF environment, ROS production paralleled LDH values, as gauged by a substantial decrease versus the media environment. Following exposure to  $25 \mu\text{g ml}^{-1}$  AgNPs, intracellular ROS levels were reduced from 188%

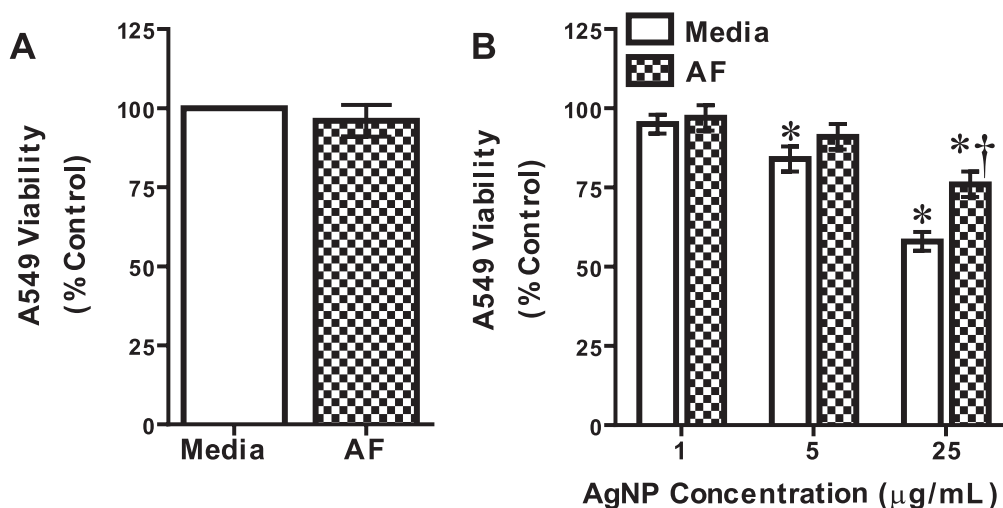


**Figure 5.** AgNP-induced cytotoxicity varied between media and AF environments. (A) To ensure that AF did not induce a cytotoxic response in the A549 model, viability was determined following a 24 h exposure in either media or AF. (B) Following a 24 h exposure to AgNPs at varying concentrations, A549 cells underwent evaluation for cytotoxicity as assessed via LDH release [38]. Data represents three independent trials with \* and † indicating statistical significance from an untreated media control and between fluids, respectively ( $p < 0.05$ ).

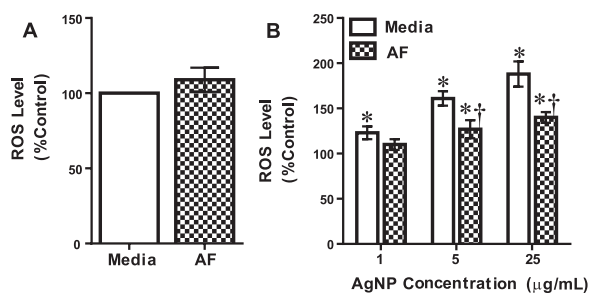


**Figure 6.** Evaluation of intracellular ROS levels in media and AF. (A) Fluid specific controls were run to verify that incubation in AF did not produce ROS in A549 cells. (B) Following a 24 h exposure to AgNPs in the denoted fluid, intracellular stress was monitored through ROS production. Data represents three independent trials with \* and † indicating statistical significance from an untreated media control and between fluids, respectively ( $p < 0.05$ ).

within media to 140% in an AF environment. Taken together, the cytotoxicity and stress responses demonstrated that the inclusion of physiological fluid produced differential bioreponses in an A549 model.

### 3.4. Implications of these results

Owing to their potential to serve as a powerful tool, this study further supports efforts to implement artificial physiological fluids in the safety assessment and efficacy screening of NPs and nano-based applications. Of particular interest is implementing relevant fluids to characterize and evaluate the behavior of NPs as they progress through the biological life cycle. Tracking changes to NP physicochemical properties throughout their lifespan is an emerging area of interest due to the recognition that environmental factors, such as fluid composition, are capable of modifying critical parameters and behaviors [39, 40]. This study targeted an alveolar exposure region, which in addition to serving as a major route of NP exposure, has been correlated with extensive NP retention

[41, 42]. Human alveolar epithelial cells (A549) were employed, in addition to AF and LF, which represent the likely environments AgNPs would encounter post inhalation *in vivo*.

This work is unique with respect to the fact that it examined the impact of modified exposure scenarios on AgNPs physicochemical properties, the nano-cellular interface, and their subsequent biological responses. When the PVP-coated AgNPs were dispersed in AF, they underwent a significant transformation, including increased agglomeration, modified surface charge, and a drop in ionic dissolution. As ions are formed from the free surface of NP agglomerates, the increase in particle aggregation was the leading cause for the observed reduction in ion production: as the surface area to volume ratio is inversely proportional to size. Deposition analysis showed that the AF-dependent modest increase in AgNP agglomeration did result in higher A549 internalization, due to greater sedimentation forces. However, even though the cells were associated with a higher NP mass, exposure within AF mitigated the toxic potential of AgNPs, as assessed via viability and ROS production. While these results may initially seem counterintuitive, they are in agreement with the reduction of silver ion generation; which has been directly correlated to cytotoxicity [16, 17]. Therefore, while both deposition and ionic dissolution are known to impact the biocompatibility of NPs, the decrease in ion generation was not fully counteracted by the slight increase in AgNP delivery.

Understanding the impact of biological fluids on NPs properties is beneficial to the scientific community as physicochemical parameters have been directly correlated to nanotoxicological outcomes [43]. Artificial physiological fluids are advantageous due to the fact that they provide a means for NP exposure within a biologically representative environment and allow for particle recollection post-exposure. Currently, it is exceptionally challenging to recover NPs from animal models, making it near impossible to evaluate

their modifications *in vivo*. New techniques are emerging, such as the visualization and analysis of gold NPs in skin biopsies [44], however the range of available characterization assessments via this mechanism are extremely limited. To date, the majority of studies have identified extensive NP agglomeration following dispersion in varying biological fluids [36, 39, 40]. This aggregation arises due to the high salt content, which mimics true physiological environments and is therefore more representative of *in vivo* models [45, 46].

Fluid-specific agglomeration introduces several other implications and system modifications. For example, in non-acidic environments, such as alveolar and interstitial fluids, augmented agglomeration can reduce ionic dissolution, owing to a decrease in the NP surface area to volume ratio [27, 39]. This phenomena was confirmed in this study and introduced significant implications for AgNPs, specifically, as the production of ions is a well-documented mechanism of nanotoxicity [16, 17]. However, in acidic environments, such as LF, the rate of ionic dissolution can increase, and has been shown to initiate a second round of AgNP-dependent cytotoxicity [47]. Beyond modifying ionic dissolution, NP agglomeration can modify biological transport mechanisms, as these aggregates will sediment out of solution more easily. For nano-based applications that are highly dependent upon effective delivery, such as drug delivery and bio-imaging, fluid-dependent alterations to transport may be a limiting factor in application efficacy.

In addition to potentially limiting application efficacy, the formation of large aggregates and greater sedimentation will directly impact the nano-cellular interface through increasing deposition [19, 28]. As NP interactions have been correlated directly to observed nanotoxicological profiles, fluid-dependent deposition increases could induce bioeffects not identified within a traditional *in vitro* model. For example, Braun *et al* [19] uncovered a previously unseen increase in gold nanosphere cytotoxicity when NPs were exposed to keratinocytes within an interstitial fluid environment. However, as shown in this study, there are frequently multiple contributing factor to NP-induced cellular responses, such as combining deposition with the rate of ionic dissolution. Therefore, a traditional *in vitro* model may not be able to accurately capture these numerous influences. One considerable drawback associated with traditional *in vitro* models is the lack of physiological relevance, which results in poor correlations and conflicting results between *in vitro* and *in vivo* assessments [48, 49]. For example, a recent study identified that polymeric NPs induced cytotoxicity within an *in vitro* model, but uncovered no discernable responses within rats [20]. As such, implementing physiological fluids may be a means to overcome these limitations and improve the biological relevance of *in vitro* models, thereby making assessments more predictive.

#### 4. Conclusions

The goal of this study was to analyze the life cycle of AgNPs following inhalation through the utilization of multiple,

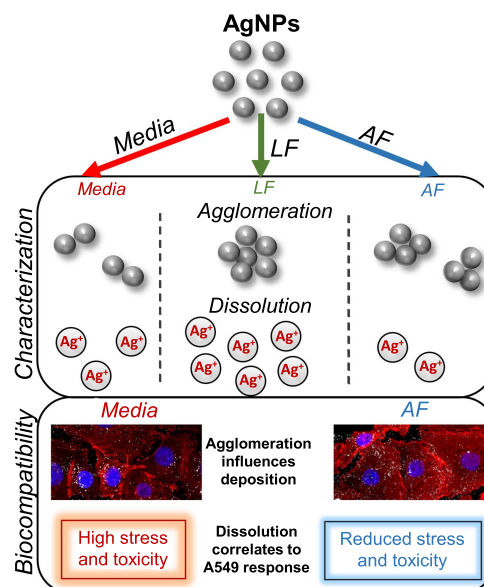


**Figure 7.** Summary of results. This study identified that both AF and LF altered AgNP characterization, including agglomeration and ionic dissolution. Additionally, when AgNPs were introduced into A549 cells within an AF environment, modification to the nano-cellular interface and biological responses were identified.

representative physiological fluids (alveolar and lysosomal) and a human alveolar model. AgNP properties and behaviors were characterized within the fluids, as well as subsequent induced biological responses following exposure. The results of these characterization, cellular interactions, and biocompatibility studies are summarized in figure 7. Following dispersion in AF and LF, AgNP extent of agglomeration and rate of ionic dissolution were modified, though not to equal extents as each fluid introduced unique variations. When AgNPs were introduced to A549s within an AF environment, morphological modifications were observed, in addition to increased deposition. It is hypothesized that the observed rise in deposition efficiency was due to particle agglomeration, which influenced sedimentation forces. Moreover, within AF the A549 cells displayed lower stress and cytotoxicity rates following AgNP exposure, due to a reduction in ionic dissolution, which is known to be an inducer of nano-silver toxicity. The fluid-dependent increase in agglomeration resulted in a lower surface area to volume ratio in AF, ultimately reducing ion production and AgNP-induced cytotoxicity. Taken together, this work demonstrated the impact and value of incorporating physiological fluids into *in vitro* models, as these biological fluids improve exposure relevance and, ultimately, may assist in the development of better predictive modeling capabilities.

#### Acknowledgments

This research was funded in part by the National Science Foundation, award 1650960. EKB and KEB were funded by the Dayton Area Graduate Studies Institute. We would like to

thank Ms Elizabeth Maurer-Gardner for carrying out the TEM analysis.

## ORCID iDs

Kristen K Comfort  <https://orcid.org/0000-0002-4865-1342>

## References

- [1] Hussain S M, Warheit D B, Ng S P, Comfort K K, Grabinski C M and Braydich-Stolle L K 2015 At the crossroads of nanotoxicology *in vitro*: past achievements and current challenges *Toxicol. Sci.* **147** 5–16
- [2] Gupta N, Fischer A R and Frewer L J 2015 Ethics, risk and benefits associated with different applications of nanotechnology: a comparison of expert and consumer perceptions of drivers of social acceptance *Nanoethics* **9** 93–108
- [3] Ge L, Li Q, Wang M, Ouyang J, Li X and Xing M M Q 2014 Nanosilver particles in medical applications: synthesis, performance, and toxicity *Int. J. Nanomedicine* **9** 2399–407
- [4] Eleonore F and Salar-Behzadi S 2014 Toxicological assessment of inhaled nanoparticles: role of *in vivo*, *ex vivo*, *in vitro*, and *in silico* studies *Int. J. Mol. Sci.* **15** 4795–822
- [5] Yah C S, Simate G S and Iyuke S E 2012 Nanoparticles toxicity and their routes of exposures *Pak. J. Pharm Sci.* **25** 477–91
- [6] Mackey M A, Ali M R K, Austin L R, Naer R D and El-Sayed M A 2014 The most effective gold nanorod size for plasmonic photothermal therapy: theory and *in vitro* experiments *J. Phys. Chem. B* **118** 1319–26
- [7] Zhang X 2015 Gold nanoparticles: recent advances in biomedical applications *Cell Biochem. Biophys.* **72** 771–5
- [8] Prabhu S and Poulouse E K 2012 Silver nanoparticles: mechanism of antimicrobial action, synthesis, medical applications, and toxicity effects *Int. Nano Lett.* **2** 32
- [9] Aioub M, Kang B, Mackey M A and El-Sayed M A 2014 Biological targeting of plasmonic nanoparticles improves cellular imaging via enhanced scattering in the aggregates formed *J. Phys. Chem. Lett.* **5** 2555–61
- [10] Ahamed M, AlSalhi M S and Siddiqui M K J 2010 Silver nanoparticle applications and human health *Clin. Chim. Acta* **411** 1841–8
- [11] Comfort K K, Braydich-Stolle L K, Maurer E I and Hussain S M 2014 Less is more: long-term *in vitro* exposure to low levels of silver nanoparticles provides new insights for nanomaterial evaluation *ACS Nano* **8** 3260–71
- [12] Makama S, Kloet S K, Piella J, van den Berg H, de Ruijter N C A, Puentes V F, Rietjens I M C M and van den Brink N W 2018 Effects of systematic variation in size and surface coating of silver nanoparticles on their *in vitro* toxicity to macrophage RAW 264.7 cells *Toxicol. Sci.* **162** 79–88
- [13] Ivask A *et al* 2014 Size-dependent toxicity of silver nanoparticles to bacteria, yeast, algae, crustaceans and mammalian cells *in vitro* *PLoS One* **9** e102108
- [14] Braakhuis H M, Gosens I, Krystek P, Boere J A, Cassee F R, Fokkens P H, Post J A, van Loveren H and Park M V 2014 Particle size dependent deposition and pulmonary inflammation after short-term inhalation of silver nanoparticles *Part. Fibre Toxicol.* **11** 49
- [15] Kang M, Lim C H and Han J H 2013 Comparison of toxicity and deposition of nano-sized carbon black aerosol prepared with or without dispersing sonication *Toxicol. Res.* **29** 121–7
- [16] Garg S, Rong H, Miller C J and Waite T D 2016 Particle size dependent deposition and pulmonary inflammation after short-term inhalation of silver nanoparticles *Environ. Sci. Technol.* **50** 3890–6
- [17] Comfort K K, Maurer E I and Hussain S M 2014 Slow release of ions from internalized silver nanoparticles modifies the epidermal growth factor signaling response *Colloids Surf. B* **123** 136–42
- [18] Goodman T T, Ng C P and Pun S H 2008 3D tissue culture systems for the evaluation and optimization of nanoparticle-based drug carriers *Bionconj. Chem.* **19** 1951–9
- [19] Braun N J, DeBrosse M C, Hussain S M and Comfort K K 2016 Modification of the protein corona-nanoparticle complex by physiological factors *Mater. Sci. Eng. C* **64** 34–42
- [20] Voigt N, Henrich-Noack P, Kockentiedt S, Hintz W, Tomas J and Sabel B A 2014 Toxicity of polymeric nanoparticles *in vivo* and *in vitro* *J. Nanopart. Res.* **16** 2379
- [21] Arora S, Rajwade J M and Paknikar K M 2012 Nanotoxicology and *in vitro* studies: the need of the hour *Toxicol. Appl. Pharmacol.* **258** 151–65
- [22] Nel A, Xia T, Meng H, Wang X, Lin S, Ji Z and Zhang H 2013 Nanomaterial toxicity testing in the 21st century: use of a predictive toxicological approach and high-throughput *Acc. Chem. Res.* **46** 607–21
- [23] Clift M J D, Gehr P and Rothen-Rutishauser B R 2011 Nanotoxicology: a perspective and discussion of whether or not *in vitro* testing is a valid alternative *Arch. Toxicol.* **85** 723–31
- [24] Shukla R, Bansal V, Chaudhary M, Basu A, Bhonde R R and Sastry M 2005 Biocompatibility of gold nanoparticles and their endocytic fate inside the cellular compartment: a microscopic overview *Langmuir* **21** 10644–54
- [25] Untener E A, Comfort K K, Maurer E I, Grabinski C M, Comfort D A and Hussain S M 2013 *ACS Appl. Mater. Interfaces* **5** 8366–73
- [26] Choi S J, Lee J K, Jeong J and Choy J H 2013 Toxicity evaluation of inorganic nanoparticles: considerations and challenges *Mol. Cell. Toxicol.* **9** 205–10
- [27] Comfort K K, Speltz J W, Stacy B M, Dosser L R and Hussain S M 2013 Physiological fluid specific agglomeration patterns diminish gold nanorod photothermal characteristics *Adv. Nanopart.* **2** 336–43
- [28] Breitner E K, Hussain S M and Comfort K K 2015 The role of biological fluid and dynamic flow in the behavior and cellular interactions of gold nanoparticles *J. Nanobiotechnol.* **13** 56
- [29] Cathe D S, Whitaker J N, Breitner E K and Comfort K K 2017 Exposure to metal oxide nanoparticles in physiological fluid induced synergistic biological effects in a keratinocyte model *Toxicol. Lett.* **268** 1–7
- [30] Stopford W, Turner J, Cappellini D and Brock T 2003 Bioaccessibility testing of cobalt compounds *J. Environ. Monit.* **5** 675–80
- [31] Tejamaya M, Romer I, Merrifield R C and Lead J R 2012 Stability of citrate, PVP, and PEG coated silver nanoparticles in ecotoxicology media *Environ. Sci. Technol.* **46** 7011–7
- [32] Luby A O, Breitner E K and Comfort K K 2016 Preliminary protein corona formation stabilizes gold nanoparticles and improves deposition efficiency *Appl. Nanosci.* **6** 827–36
- [33] Nguyen V H and Lee B J 2017 Protein corona: a new approach for nanomedicine design *Int. J. Nanomed.* **12** 3137–51
- [34] Loza K, Diendorf J, Sengstock C, Ruiz-Gonzalez L, Gonzalez-Calbet J M, Vallet-Regi M, Koller M and Epple M 2014 The dissolution and biological effects of silver

- nanoparticles in biological media *J. Mater. Chem. B* **2** 1634–43
- [35] Semisch A, Ohle W, Witt B and Hartwig A 2014 Cytotoxicity and genotoxicity of nano—and microparticulate copper oxide: role of solubility and intracellular bioavailability *Part. Fibre Toxicol.* **11** 10
- [36] Markus A A, Parson J R, Roex E W M, de Voogt P and Laane R W P M 2015 Modeling aggregation and sedimentation of nanoparticles in the aquatic environment *Sci. Tot. Environ.* **506** 323–9
- [37] Braydich-Stolle L K, Breitner E K, Comfort K K, Schlager J J and Hussain S M 2014 Dynamic characteristics of silver nanoparticles in physiological fluid: toxicological implications *Langmuir* **30** 15309–16
- [38] Smith S M, Wunder M B, Norris D A and Shellman Y G 2011 A simple protocol for using a LDH-based cytotoxicity assay to assess the effects of growth and death inhibition at the same time *PLoS One* **6** e26908
- [39] Stebounova L V, Guio E and Grassian V H 2011 Silver nanoparticles in simulated biological media: a study of aggregation, sedimentation, and dissolution *J. Nanopart. Res.* **13** 233–44
- [40] Cho W S, Duffin R, Howie S E, Scotton C J, Wallace W A, Macnee W, Bradley M, Megson I L and Donaldson K 2011 Progressive severe lung injury by zinc oxide nanoparticles; the role of  $Zn^{2+}$  dissolution inside lysosomes *Part. Fibre Toxicol.* **8** 27
- [41] Geiser M and Kreyling W G 2010 Deposition and biokinetics of inhaled nanoparticles *Part. Fibre Toxicol.* **7** 2
- [42] Fireman E, Edelheit R, Stark M and Shai A B 2017 Differential pattern of deposition of nanoparticles in the airway of exposed workers *J. Nanopart. Res.* **19** 30
- [43] Shin S W, Song I H and Um S H 2015 Role of physicochemical properties in nanoparticle toxicity *Nanomaterials* **5** 1351–65
- [44] Sykes E A, Dai Q, Tsoi K M, Hwang D M and Chang W C W 2014 Nanoparticle exposure in animals can be visualized in the skin and analyzed via skin biopsy *Nat. Commun.* **5** 3796
- [45] Sethi M, Joung G and Knecht M R 2009 Stability and electrostatic assembly of Au nanorods for use in biological assays *Langmuir* **25** 317–25
- [46] Vasicek T W, Jenkins S V, Vaz L, Chen J and Stenken J A 2017 Thermoresponsive nanoparticle agglomeration/aggregation in salt solutions: dependence on graft density *J. Colloid Interface Sci.* **506** 338–45
- [47] Sabella S *et al* 2014 A general mechanism for intracellular toxicity of metal-containing nanoparticles *Nanoscale* **6** 7052–61
- [48] Demokritou P *et al* 2013 An *in vivo* and *in vitro* toxicological characterization of realistic nanoscale  $CeO_2$  inhalation exposures *Nanotoxicology* **7** 1338–50
- [49] Frohlich E and Salar-Behzadi S 2014 Toxicological assessment of inhaled nanoparticles: role of *in vivo*, *ex vivo*, *in vitro*, and *in silico* studies *Int. J. Mol. Sci.* **15** 4795–822